Science Advances
AAAS

advances.sciencemag.org/cgi/content/full/6/50/eaba8237/DC1

Supplementary Materials for

Ceramide chain length–dependent protein sorting into selective endoplasmic reticulum exit sites

Sofia Rodriguez-Gallardo, Kazuo Kurokawa*, Susana Sabido-Bozo, Alejandro Cortes-Gomez, Atsuko Ikeda, Valeria Zoni, Auxiliadora Aguilera-Romero, Ana Maria Perez-Linero, Sergio Lopez, Miho Waga, Misako Araki, Miyako Nakano, Howard Riezman, Kouichi Funato, Stefano Vanni, Akihiko Nakano, Manuel Muñiz*

*Corresponding author. Email: kkurokawa@riken.jp (K.K.); mmuniz@us.es (M.M.)

Published 11 December 2020, *Sci. Adv.* **6**, eaba8237 (2020)
DOI: 10.1126/sciadv.aba8237

The PDF file includes:

Other Supplementary Material for this manuscript includes the following:

(available at advances.sciencemag.org/cgi/content/full/6/50/eaba8237/DC1)

Fig. S1

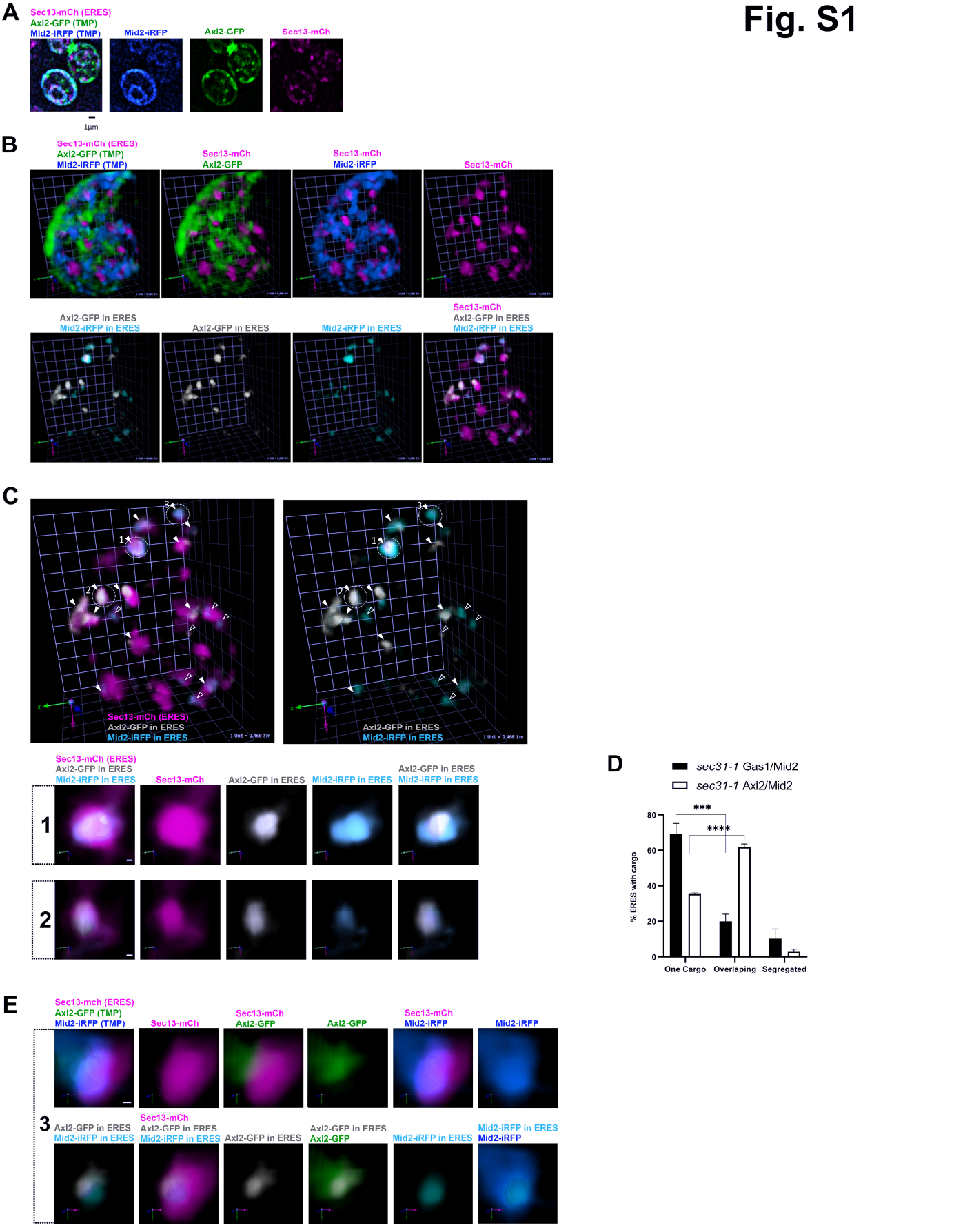
A
Sec13-mCh (ERES)
Axl2-GFP (TMP)
Mid2-iRFP (TMP)
Mid2-iRFP
Axl2-GFP
Sec13-mCh
1µm
B
Sec13-mCh (ERES)
Axl2-GFP (TMP)
Mid2-iRFP (TMP)
Sec13-mCh
Axl2-GFP
Sec13-mCh
Mid2-iRFP
Sec13-mCh
Axl2-GFP in ERES
Mid2-iRFP in ERES
Axl2-GFP in ERES
Mid2-iRFP in ERES
Sec13-mCh
Axl2-GFP in ERES
Mid2-iRFP in ERES
C
Sec13-mCh (ERES)
Axl2-GFP in ERES
Mid2-iRFP in ERES
Axl2-GFP in ERES
Mid2-iRFP in ERES
Sec13-mCh (ERES)
Axl2-GFP in ERES
Mid2-iRFP in ERES
Sec13-mCh
Axl2-GFP in ERES
Mid2-iRFP in ERES
Axl2-GFP in ERES
Mid2-iRFP in ERES
1
2
D
sec31-1 Gas1/Mid2
sec31-1 Axl2/Mid2
***
****
% ERES with cargo
80
60
40
20
0
One Cargo
Overlaping
Segregated
E
Sec13-mch (ERES)
Axl2-GFP (TMP)
Mid2-iRFP (TMP)
Sec13-mCh
Sec13-mCh
Axl2-GFP
Axl2-GFP
Sec13-mCh
Mid2-iRFP
Mid2-iRFP
3
Axl2-GFP in ERES
Mid2-iRFP in ERES
Sec13-mCh
Axl2-GFP in ERES
Mid2-iRFP in ERES
Axl2-GFP in ERES
Axl2-GFP in ERES
Axl2-GFP
Mid2-iRFP in ERES
Mid2-iRFP in ERES
Mid2-iRFP

Fig. S1. Different transmembrane cargos are recruited to the same ERES. *sec31-1* cells expressing galactose-inducible transmembrane secretory cargos, Axl2-GFP (TMP, green) and Mid2-iRFP (TMP, blue), and constitutive ERES marker Sec13-mCherry (ERES, magenta) were incubated at 37ºC for 30 min and then shifted down to 24°C for releasing secretion block and imaged by SCLIM after 20 min. (A) Representative merged or individual 2D projection images (10 z sections) of cargo and ERES markers are shown. Scale bar, 1 μm. (B) Upper panels show representative merged or individual 3D cell hemisphere images of cargos and ERES marker. Lower panels show the same images as that in upper panels but processed to display only the cargo (Axl2-GFP, yellow, and Mid2-iRFP, light blue) present in the ERES (Sec13-mCh, magenta). Scale unit, 0.450 μm. (C) Representative merged 3D image processed as in the lower panel in (B). The white filled arrowheads mark ERES with overlapping cargo. The open arrowheads mark ERES containing only one cargo. Right panels show processed merged or individual enlarged 3D images of selected ERES with overlapping cargos marked in (C). Scale bar, 100 nm. (D) Quantification of several micrographs described in (C). The graph plots the average percentage of ERES containing only one cargo, segregated cargos and overlapping cargos in *sec31-1* expressing Gas1-GFP and Mid2-iRFP, or Axl2-GFP and Mid2-iRFP. n = 432 in 54 cells (Gas1-GFP and Mid2-iRFP) and n = 310 in 41 cells (Axl2-GFP and Mid2-iRFP) in three independent experiments. Error bars indicate the SD. Statistics: two-tailed, unpaired t-test. ***P = 0.0002 (Gas1-GFP and Mid2-iRFP) and ****P < 0,0001 (Axl2-GFP and Mid2-iRFP). (E) The panel 4 displays merged or individual enlarged 3D images of a selected ERES marked in (C), which show that Axl2-GFP (green) and Mid2-iRFP (blue) approach the same ERES (magenta) from the same side and stay in the same restricted zone within the ERES. Scale bar, 100 nm.

Fig. S2

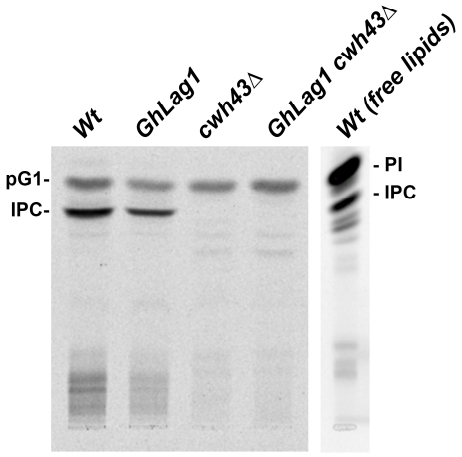

Fig. S2. In GhLag1 strain, C26 ceramide is preferentially incorporated into the GPI anchors of GPI-APs by the ceramide remodelase Cwh43. Wild-type, GhLag1, *cwh43Δ* and GhLag1 *cwh43Δ* strains were labeled with [^{3}H] *myo*-inositol for 2hr at 25ºC. The labeled PI moieties were prepared from GPI-APs and analyzed by thin-layer chromatography using the solvent system (55:45:10 chloroform-methanol-0.25% KCl). Lipids extracted from wild-type cells (free lipids) were used as a standard. pG1, phosphatidylinositol with a C26:0 fatty acid in sn-2 position; IPC, inositolphosphorylceramide. PI, phosphatidylinositol

Fig. S3

KN; lysine-asparagine
EtN ethanolamine
P phosphate
mannose
glucosamine
inositol

proposed GPI-glycan structures monoisotopic masses of each GPI-glycan	relative abundances (%) of each GPI-glycan	
	WT	**GhLag1**
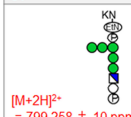 $[M+2H]^{2+}$ = 799.258 ± 10 ppm	**94.0%**	**93.1%**
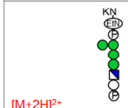 $[M+2H]^{2+}$ = 718.232 ± 10 ppm	**4.2%**	**6.1%**
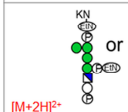 $[M+2H]^{2+}$ = 779.736 ± 10 ppm	**1.8%**	**0.8%**
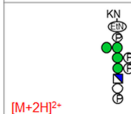 $[M+2H]^{2+}$ = 841.240 ± 10 ppm	**0.0%**	**0.0%**

Fig. S3. The GPI-glycan of Gas1-GFP is normally remodeled in the GhLag1 strain as in wild-type. The table shows the percentage of different GPI-glycan structures found in Gas1-GFP immunoprecipitated from wild-type and GhLag1 cells. The relative abundance (%) of each GPI-glycan was calculated from the peak intensity of monoisotopic masses of each GPI-glycan in extracted ion chromatogram using Xcalibur software ver. 2.2. (Thermo Fisher Scientific). These structures contain GPI peptides (KN) bearing hexosamine (glucosamine) attached to Man1 as reported previously (*30*).

Fig. S4

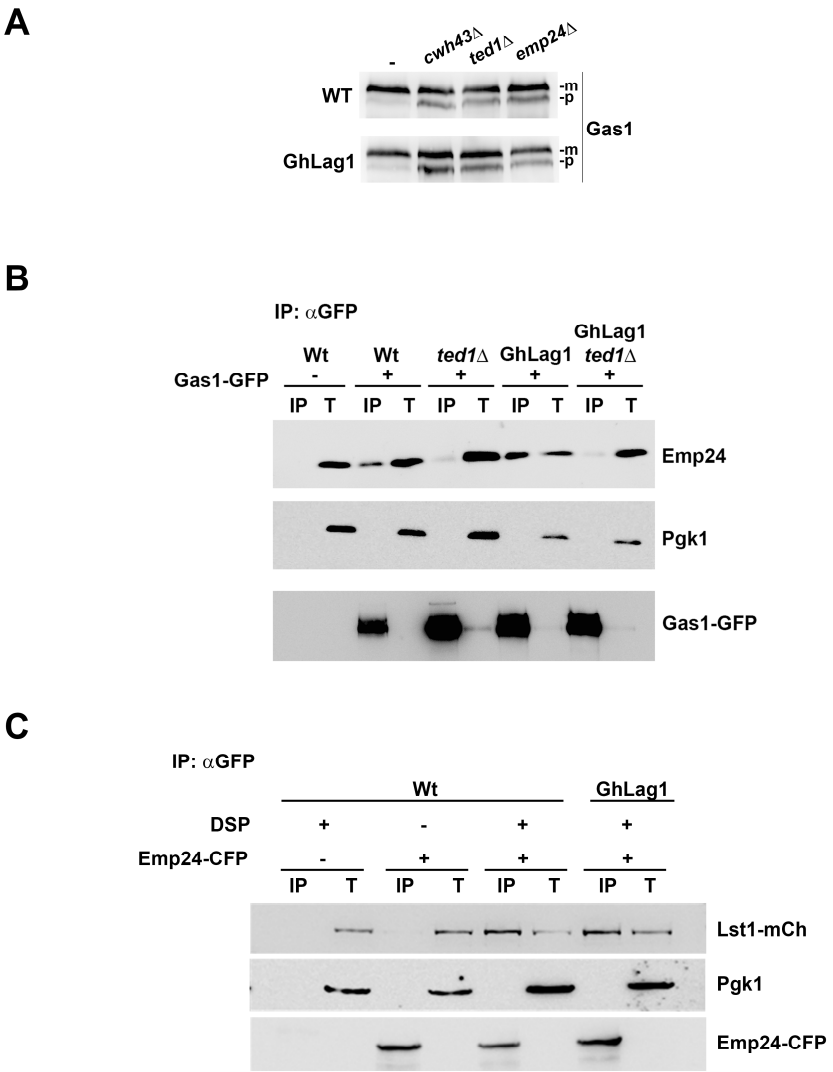

Fig. S4. C26 ceramide-based clustering does not entail differential interactions of the components of the specialized GPI-AP ER export machinery. (A) Analysis of the specific requirements for Gas1 transport in GhLag1 strain. ER-to-Golgi transport of Gas1 expressed in the strain GhLag1 requires the activities of the ceramide remodelase Cwh43, the GPI-glycan remodelase Ted1 and the cargo receptor p24 complex because *cwh43*Δ GhLag1, *ted1*Δ GhLag1 and *emp24*Δ GhLag1 mutant cells accumulate the precursor ER form of Gas1. Such requirements indicate that, in GhLag1 cells, Gas1 is remodeled with ceramide and exported from the ER by the p24 complex trough the remodeled GPI-glycan. Western blot analysis for Gas1 of cell extracts prepared from wild-type and GhLag1 strains bearing different deletions. ER (p) and Golgi (m) Gas1p forms are indicated. (B) Co-immunoprecipitation (IP) assay between Gas1-GFP and the p24 complex subunit Emp24. Gas1-GFP expressed in GhLag1 strain is specifically recognized by the p24 complex in a Ted1-dependent manner. This physical interaction is specific because Pgk1, an unrelated cytosolic protein, is not recovered after Gas1-GFP IP. Enriched ER fractions of wild-type and GhLag1 strains without and with *ted1Δ* deletion expressing Gas1-GFP were solubilized and analyzed by native

immunoprecipitation (IP) with anti-GFP antibody followed by immunoblotting (IB) with anti-Emp24 and anti-Pgk1 antibodies. Totals (T) represent a fraction of the solubilized input material. (C) Crosslinking assay between Lst1-mCherry and Emp24-CFP. Lst1-mCherry is efficiently recruited by the p24 complex in GhLag1 strain. Extracts of wild-type and GhLag1 strains expressing Emp24-CFP and Lst1-mCherry were incubated with (+) and without the crosslinker DSP, solubilized, and immunoprecipitated with anti-GFP antibody, followed by IB with anti-mCherry and Pgk1 antibodies. Totals (T) represent a fraction of the solubilized input material.

Fig. S5

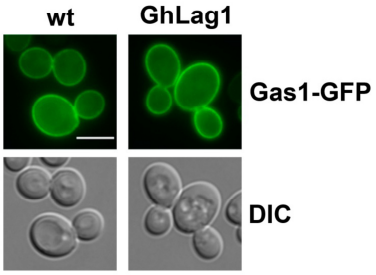

Fig. S5. Gas1 is exported from the ER towards the plasma membrane in GhLag1 strain. Gas1-GFP localizes at the plasma membrane of GhLag1 cells. Live images of wild-type and GhLag1 cells expressing Gas1-GFP at 24ºC. The scale bar, 5 μm.

Fig. S6

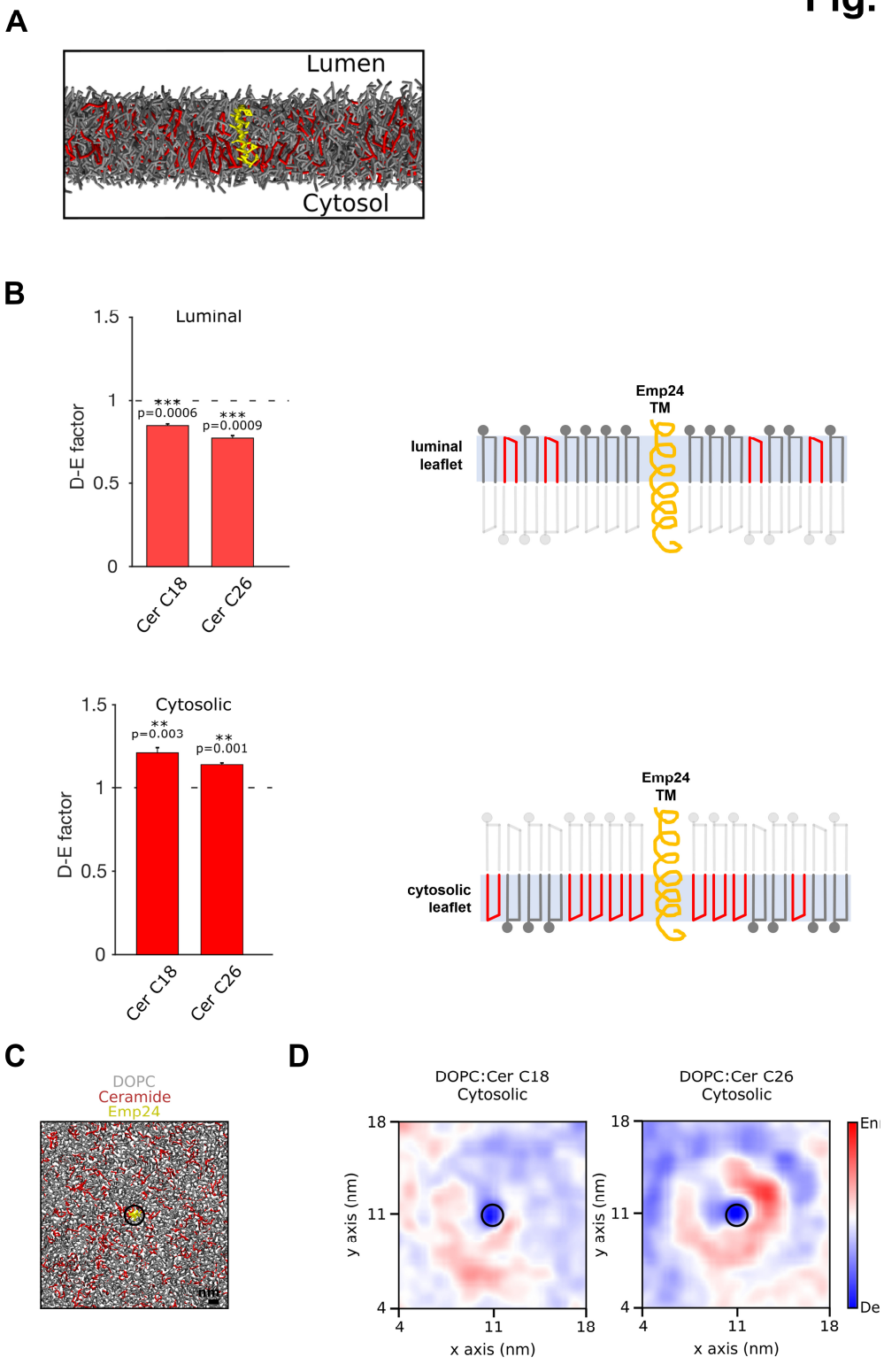

Fig. S6. Ceramides are enriched around the cytosolic portion of Emp24 TM. (A) Molecular dynamics (MD) simulation. Representative snapshot of the lateral view of the

lipid bilayer system, containing DOPC (gray) and ceramide (red) with the Emp24 transmembrane (TM) domain (yellow) spanning the bilayer. (B) Quantitative analysis of the distribution of ceramide C18 (Cer C18) or C26 (Cer C26) around the Emp24 TM in the luminal leaflet (upper graph) or in the cytosolic leaflet (lower graph) of DOPC:Cer bilayers, resulting from the MD simulations. The graphs plot the Depletion-Enrichment (D-E) factor which indicates ceramide depletion around the Emp24 TM for values below 1 or ceramide enrichment for values above 1. The D-E analysis shows that both C18 and C26 ceramides are depleted around the luminal portion of Emp24 TM but enriched with similar preferences around the cytosolic portion of Emp24 TM. The cartoons represent the D-E analysis for each considered membrane leaflet (DOPC gray, ceramides red). (C) Representative snapshot of the top view of the lipid bilayer system (cytosolic side), containing DOPC (gray), ceramide (red) and Emp24 TM (yellow). The black ring represents the outermost radius of Emp24 and it indicates the position of the protein in the simulations/analysis. (D) Top view D-E map for Cer18 or Cer26 around the Emp24 TM (black ring) in the cytosolic leaflet of DOPC:Cer bilayers, resulting from the MD simulations. The maps are obtained as average over 4 replicas.

Table S1. Strains of *Saccharomyces cerevisiae* used for this study.

Strain	Relevant genotype	Source
MMY1583	MATα *sec31-1 SEC13-mCherry::TRP1 GALp-MID2-iRFP::URA3 leu2 his3 ade2*	This study
MMY1635	MATa *sec31-1 SEC13-mCherry::TRP1 lag1Δ::HIS3 lac1Δ::ADE2 TDH3::GhLAG1::TRP1 GALp-MID2-iRFP::URA3 leu2*	This study
RH2874	MATα *leu2 lys2 trp1 ura3*	H. Riezman
MMY870	MATa *cwh43Δ::KanMx leu2 his3 ade2 trp1 ura3*	This study
MMY1192	MATa *ted1Δ::KanMx leu2 his3 ade2 trp1 ura3*	This study
RH1961	MATa *emp24Δ::LEU2 leu2 his4 ura3 bar1*	H. Riezman
RH6979	MATα *lag1Δ::HIS3 lac1Δ::ADE2 TDH3::GhLAG1::TRP1 leu2 ura3*	H. Riezman
MMY1659	MATα *cwh43Δ::KanMx lag1Δ::HIS3 lac1Δ::ADE2 TDH3::GhLAG1::TRP1 leu2 ura3*	This study
MMY1661	MATα *ted1Δ::KanMx lag1Δ::HIS3 lac1Δ::ADE2 TDH3::GhLAG1::TRP1 leu2 ura3*	This study
RH6986	MATα *emp24Δ::KanMx lag1::HIS3 lac1::ADE2 GPD-Flag-GhLAG1::TRP1 leu2 ura3*	H. Riezman
MMY1594	MATα *sec31-1 SEC13-mCherry::TRP1 emp24Δ*::Hph *ura3 leu2 his3 ade2*	This study
MMY1658	MATa *sec31-1 SEC13-mCherry::TRP1 ted1Δ::KanMx ura3 leu2 ade2*	This study
MMY1758	MATα *sec31-1 SEC13-mCherry::TRP1 lst1Δ::KanMx ura3 leu2 his3 ade2*	This study
RH7058	MATa *LST1-mCherry::kanMx ura3 leu2 his3 trp1*	H. Riezman
MMY1745	MATα *LST1-mCherry::kanMx lag1Δ::HIS3 lac1Δ::ADE2 TDH3::GhLAG1::TRP1 ura3 leu2*	This study

Table S2. Oligonucleotides used in this study.

Target	Primer Sequence (5'-3')
Mid2-iRFP tagged	F -AAGAAAAATTCTATGATGAACAAGGTAACGAATTATCACCA CGAAATTATGGTGACGGTGCTGGTTTA- R -TTGAGGAATGAAAAGTAGCCATAAGCACTAAATGATATGAA TGGATATGAAGCGACCAGCATTCACAT-
Mid2-iRFP insertion in pRS306-GAL promoter plasmid	F -TATTCAGCGGCCGCATGTTGTCTTTCACAACCAA- R -TATTCAGCGGCCGCATGTTGTCTTTCACAACCAA-
Gas1-GFP insertion in pBEVY-GL plasmid	F -GACTGACCCGGGATGTTGTTTAAATCCCTTTC- R -AATAGTCTCGAGTTAAACCAAAGCAAAACCGA-
Axl2-GFP insertion in pBEVY-GL plasmid	F -GCTTGAGGATCCATGACACAGCTTCAGATTTCATTATTGCTG- R -CGATTCCTGCAGCTATTTGTATAGTTCATCCATGCCATGTGT-

Movie S1.

Multi-angle 3D reconstructed movie representing data of **Fig. 1**. Newly synthesized GPI cargo Gas1-GFP (green) forms clusters in the ER membrane adjacent to specific ERES (magenta) while transmembrane cargo Mid2-iRFP (blue) is distributed throughout the ER membrane.

Movie S2.

Multi-angle 3D reconstructed movie representing data of **Fig. 2**. GPI-AP Gas1-GFP (green) is sorted into different ERES (magenta) from the transmembrane cargo Mid2-iRFP (blue) upon ER exit.

Movie S3. Multi-angle 3D reconstructed movie representing data of **Fig. S1**. Two distinct transmembrane cargos, Axl2-GFP (green) and Mid2-iRFP (blue) enter the same ERES (magenta) together.

Movie S4.

Multi-angle 3D reconstructed movie representing data of **Fig. 4**. GPI-AP Gas1-GFP (green) is not clustered and enters the same ERES (magenta) as Mid2-iRFP transmembrane cargo (blue) in the ER membrane with shorter C18-C16 ceramide.